Journal of Power Sources 258 (2014) 218–227

Contents lists available at ScienceDirect

Journal of Power Sources

journal homepage: www.elsevier.com/locate/jpowsour

Determination of lithium-ion battery state-of-health based on constant-voltage charge phase

Akram Eddahech*, Olivier Briat, Jean-Michel Vinassa

Univ. Bordeaux, IMS, UMR 5218 CNRS, IPB, F-33400 Talence, France

HIGHLIGHTS

- Experiments on calendar aging of four lithium battery technologies.
- Constant voltage (CV) charge phase data helped to determine battery state of health.
- According to technology, CV current and/or CV duration through aging are exploited.
- A simple method that can be easily implemented in a BMS.

ARTICLE INFO

Article history:
Received 5 December 2013
Received in revised form
17 January 2014
Accepted 6 February 2014
Available online 15 February 2014

Keywords:
Lithium battery
Calendar aging
CC–CV charge
Lithium intercalation
State of health

ABSTRACT

Lithium battery performances degrade even at rest time that means when electric/hybrid electric vehicles are in the parking. This phenomenon is well known as calendar aging. In this paper, the kinetic of the CC–CV charge at 1 C and mainly kinetic of the voltage regulation, CV step, is investigated as an indicator of battery state-of-health through calendar aging. In fact, CV step is responsible in a major part of lithium intercalation into negative electrode and revealed to give signification on cyclable lithium loss which is the major cause of calendar aging according to literature and post mortem analysis. Comparison from the aging of four battery technologies is presented. Through aging, results show a difference in battery behavior even if the time for CC charge is decreasing for all the battery. According to battery technology, the current during CV charge phase has been useful for lithium–nickel–manganese–cobalt-oxide, lithium–nickel–cobalt–aluminum-oxide and lithium-ion–manganese battery state-of-health determination. However, in the case of the lithium–iron–phosphate battery, simple calculation of the duration of the CV step revealed to be very accurate compared to the classic discharged capacity measurement.

1. Introduction

Lithium-ion battery is a key enabling technology in advanced transportation. There is no doubt that it represents the best solution providing very high performances in terms of energy and power densities, cycle life, safety and reliability requirement [1].

However, researchers still work in battery management systems (BMS) in order to achieve comprehensive investigation of battery dynamics and its fading mechanisms and why not simplify if possible algorithm for state of charge and state of health SOH determination [2].

On the other hand, accuracy of predicting battery useful life is necessary due to battery high costs and it could be helpful not only for manufacturers by prolonging their warranty but also for users avoiding severe failures from occurring and optimizing Li-ion battery maintenance schedules [3,4].

Several works in literature focused on aging investigation of lithium batteries. These works can be classified by the employed means for the study. For example, the frequency domain identification which is based on electrochemical impedance spectroscopy and that uses Randles equivalent electric circuit models [5]. This technique revealed to be efficient in aging sources investigation [6,7]. Using it we can decouple phenomena such as electrolyte decomposition, charge transfer and double layer capacitance, solid

* Corresponding author. Laboratoire IMS, 351 cours de la libération, Bat A31, 33400 Talence, Bordeaux, France. Tel.: +33 5 40 00 26 13; fax: +33 5 56 37 15 45.
E-mail address: akram.eddahech@ims-bordeaux.fr (A. Eddahech).

http://dx.doi.org/10.1016/j.jpowsour.2014.02.020
0378-7753/

electrolyte interface and diffusion. However, this technique could not run online.

Other works in literature focused on advanced techniques namely artificial intelligence such as neural networks and/or fuzzy logic profiting from their capability to gain knowledge of complex dynamics and its use simplicity [8]. These techniques suffer from the training step shortage as it is necessary to renew it once input variables change in addition to the update rate problem and the required powerful processing computations.

Another technique for SOH monitoring is the battery model-based parameter identification developed for on-board performances identification. According to the operating data, this method adopts optimal state algorithms such as the least square and Kalman filtering in order to identify parameters giving indications on capacity and internal resistance and then battery SOH [9–11].

Otherwise, researchers often focus on time domain investigation like internal resistance increase [12] and/or charged–discharged capacity decrease over the time [13,14]. Behind this, authors looked for aging law development based on a rich experimental dataset and that could integrate other intermediate aging conditions.

The idea behind this work is very simple, how can we use kinetic of CC–CV charge as a mean for calendar aging investigation?

Therefore based on this, we focus on the time for full charge at 1 C of four technologies of lithium batteries, with the following chemistries NMC, NCA, LMO and LFP, through periodic characterization tests. The time for galvanostatic mode (CC) and potentiostatic mode (CV) is identified respectively during aging and results are discussed. Correlation with electrochemical reaction within the battery and its structure change during aging is investigated.

2. Experimental setup and first aging observations

2.1. Calendar aging experiments and sample description

This work aims to investigate and analyze the calendar aging process of lithium-ion cells used in hybrid electric vehicles HEV and full electric vehicles EV applications. Calendar aging considers battery performances fade when they are not in use thing that could not be neglected. For example, the US fleet of vehicles is not used for driving more than 90% of a day [15].

The reported aging tests are performed on a high-power/energy lithium cells from four technologies in which the insertion material of the negative electrode is a carbon material of coke type, graphite. However, all these batteries differ with their active material in the positive electrode. For example, the 12 Ah Kokam cells are made of lithium Cobalt Manganese Nickel oxide abbreviated NMC. The high-power 7 Ah cells from SAFT are LiNiCoAl type cathode whose acronym is NCA. The 5.3 Ah cells from LG are carried out of $LiMn_2O_4$ cathode, so called LMO. Finally the 8 Ah LiFeBATT cells are prepared from lithium iron phosphate $LiFePO_4$ well known as LFP.

These batteries were stored under three different temperatures (T 30, 45 and 60 °C) in climatic chambers and three State-Of-Charges (SOC 30%, 65% and 100%) for each temperature. Therefore in the whole we investigate nine test conditions. Furthermore, three cells are used for each test condition in order to have a good reproducibility and perform post-mortem analysis. Table 1 reports the lithium battery technologies investigated in this work.

Table 1
Properties of the lithium-ion batteries tested in the calendar aging tests.

Manufacturer	Chemistry	Nominal capacity (Ah)	Nominal voltage (V)	Minimal voltage (V)	Format	Type
Kokam	NMC	12	4.2	2.7	Prismatic	Power
LGChem	LMO–NMC	5.3	4.2	2.5	Prismatic	Energy
SAFT	NCA	7	4	2.3	Cylindrical	Power
LiFeBATT	LFP	8	3.65	2	Cylindrical	Power

2.2. Performance characterization

During the whole calendar aging test, the battery SOH is monitored thanks to periodic characterizations (check-up) which are not only based on battery capacity measurements but also on a series of electrochemical impedance spectroscopy EIS at several SOC (20%, 40%, 60%, 80% and 100%) and at 25 °C. The EIS technique is one of the most promising methods for aging mechanisms investigation for lithium-ion batteries used in automotive applications [16] since it provides rich information about battery impedance for different test conditions and at various SOC values. The electrochemical measurements are performed using Biologic workstations in galvanostatic mode and the wide frequency range of 10 mHz to 10 kHz. The charged–discharged battery capacity is evaluated at 1 C. In fact, before launching check-up, battery is taken out the aging climatic chamber and is kept at 25 °C for six hours in order to achieve thermal stability. Fig. 1 shows the check-up test chronogram.

2.3. Calendar aging analysis from EIS

Focusing on calendar aging results from the periodic check-up, it was visible that the temperature and/or the SOC increase accelerated battery aging leading to significant impedance growth and a capacity loss increase. Moreover, the impact of temperature rise was greater than the SOC increase in battery aging [17].

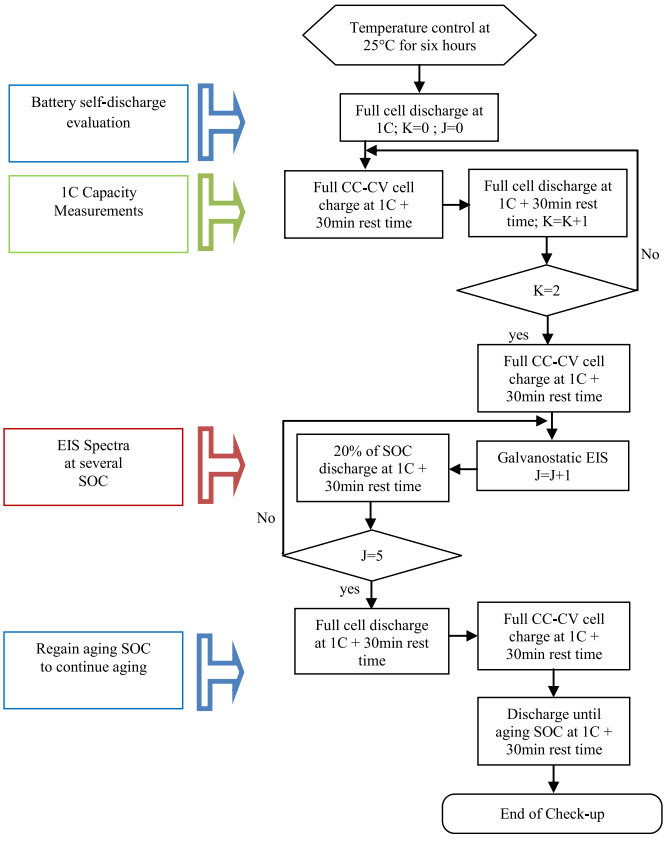

Fig. 1. Chronogram of periodic characterization protocol (check-up).

Note that according to their technology, the behavior of the battery was different through the calendar aging. When we focus on Nyquist plots issued from EIS conducted at advance aging time, several batteries (Kokam, LiFeBATT) present a single semi-circle at middle frequencies whereas the others show two semiarcs (SAFT, LGChem). In fact, all these semiarcs are expanding through aging obviously related to change in electrochemical phenomena occurring in batteries namely charge transfer, double layer capacitance and solid electrolyte interface. Thus, this confirms the dependency of the reactions within lithium battery on electrode materials and electrolyte composition. For example, from the intercept with the real axis, it was clear that the NMC and the LMO presented a higher increase of the ohmic resistances (current collector and electrolyte resistance) with aging time. However, LFP and NCA were more resistant to this.

Fig. 2 shows the Nyquist plots from EIS measurements performed at SOC 60% and 25 °C for the four battery technologies. Here we chose to represent aging of the most extreme aging conditions which are *T* 60 °C and SOC 100%.

From an electrochemical point of view, batteries performances degradation is a result of several simultaneous physicochemical processes that occur within the electrode, electrode–electrolyte interface and the electrolyte [11], even in current collector referring to recent research [18]. Overall, the aging of lithium batteries is still a very complex phenomenon. Various electrochemical processes, occurring within the cell, including intercalation of lithium ions into layered graphite anode and cathode materials, as well as mass transport of lithium ion through the electrolyte, are responsible of materials properties degradation and of the overall batteries performances drop [19,20]. Moreover, from literature, it is widely known that electrolyte decomposition and the corresponding formation of solid electrolyte interface (SEI), is the main aging process in most graphite-based lithium-ion batteries leading to an irreversible capacity loss (due to loss of active lithium) and impedance rise (due to increase in film layer thickness) [21]. This depends primarily on the electrolyte formulation and on the specific surface area of the carbon electrode [22].

3. Kinetic at constant voltage CV charge as a mean of aging investigation

3.1. CC–CV charge description

Except for Ni–MH (and Ni–Cd), all the popular battery chemistries on the market today use a form of constant current, followed

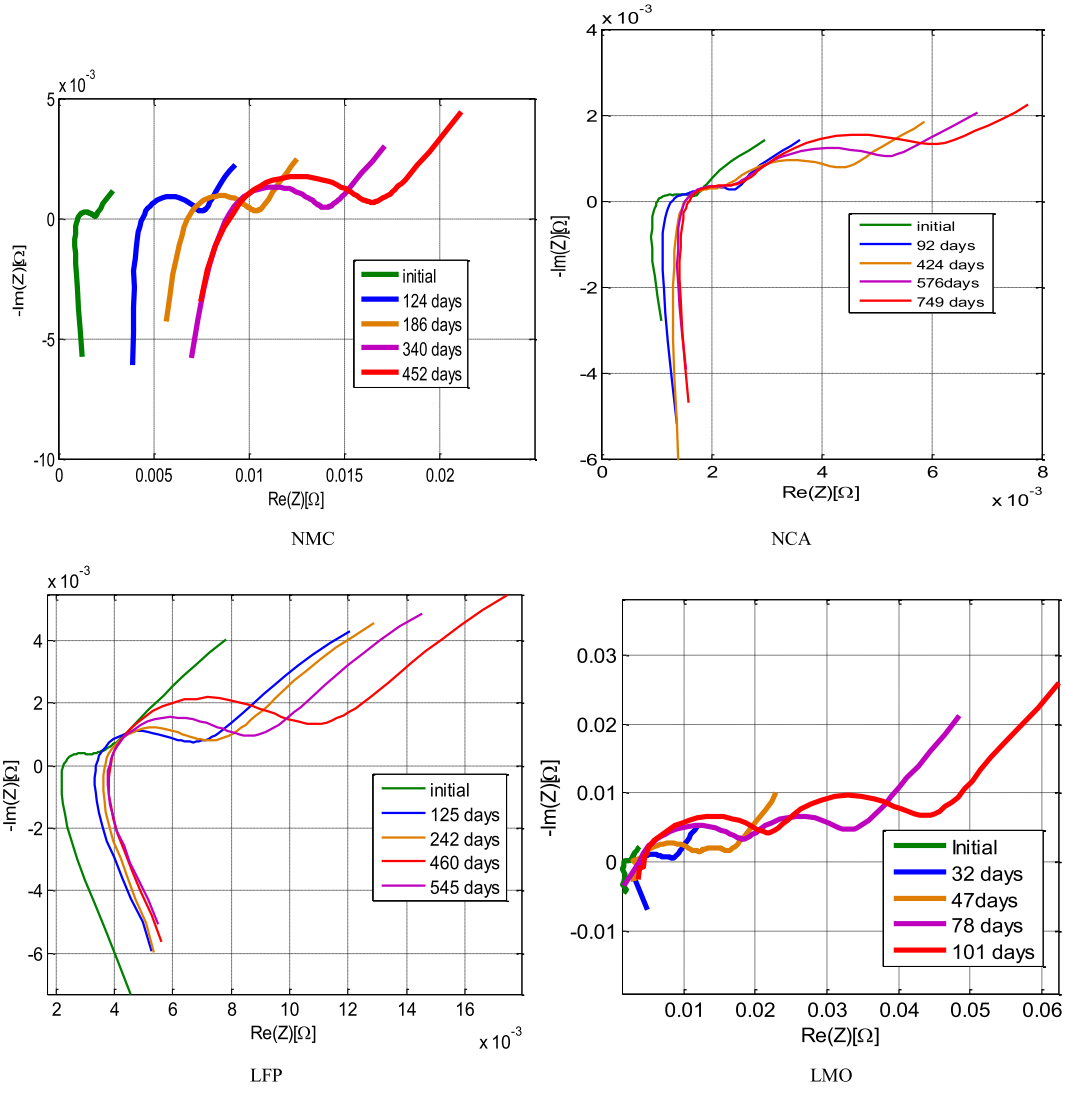

Fig. 2. Nyquist plots from characterization at several ages.

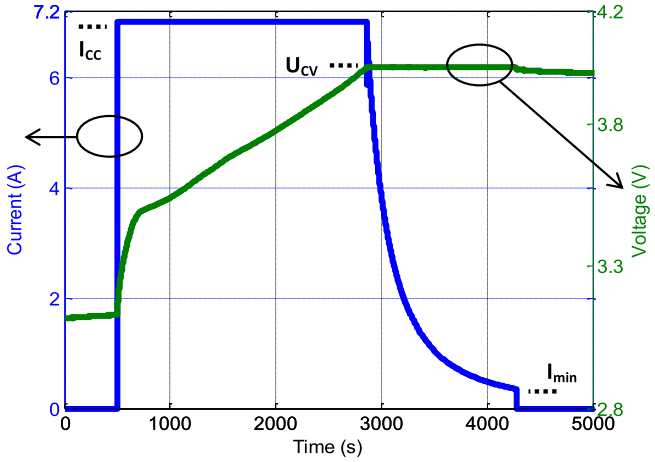

Fig. 3. CC–CV full charge of a VL6P battery at 1 C and 25 °C.

by a constant voltage charging (or constant voltage with current limit) algorithm.

The CC–CV full charge consists in two parts which are the CC step where a constant current is applied to the battery until it reaches a maximal voltage well known as the cut-off voltage. Then a CV step in which battery remains in floating mode at the cut-off voltage until the current reaches the minimum threshold generally fixed with certain fraction of the battery's maximum charge rate usually in the range of C/10 to C/30.

The graph in Fig. 3 shows the behavior of current, voltage as the charge process progresses in a VL6P cell.

As battery useful lifetime and performances are usually evaluated in term of time, we thought in why not we discover time notion in order to evaluate battery degradation? Thus in next section, we investigate time for CC–CV charge as a mean of calendar aging analysis. Therefore, we propose a method to determine battery SOH based on parameter(s) identified from the second charging phase, namely the CV phase. Thus, SOH estimation will occur within battery charging which is necessary for its normal use. So there is no need of additional measures consuming time and resources.

3.2. CV step investigation on several lithium battery technologies through aging

Figs. 4–7 show the identified time for total CC–CV charge at 1 C, the time for CC and time for CV steps during periodic check-up for the four battery technologies aged at several conditions.

On these figures, we note also capacity loss in terms of discharged capacity measured at 1 C, at 25 °C and several aging time. We always mark the maximum loss of capacity obtained. Moreover, when the loss is large, we also identify intermediate points such as singular points corresponding to the intersection of the CC and CV curves and points corresponding to a steeply variation of CV curve.

3.3. Discussion

Four battery technologies which are carried out of the following chemistry NMC, NCA, LMO and LFP respectively are studied here. Based on periodical characterization, the CC–CV charge investigation through aging reveals:

1. For all these batteries, the time for constant current step decreases with aging. This step can be viewed as similar to the discharged capacity like it is the same galvanostatic mode.
2. Global time for the CC–CV charge is constant for the NMC batteries even when batteries become aged. However, for the rest of batteries this time decreases even if the kinetic of such decrease is less visible on NCA chemistry.

As a result of the SEI reaction, the film resistance continued to increase with aging, which reduced the CC charging time due to continuous increase of the voltage drop at the interface. Moreover, the available charge amount of the cathode material decreased with aging, which also contributes the cell voltage to reach the cutoff value earlier resulting in a decrease in total charging time with Aging [23]. For the NMC battery that aging seems to clearly affect kinetic reaction because of the constant time of the global charge.

3. Time for constant voltage step increases continuously when aging of NMC and LMO batteries with a more accelerated rate once we reach advanced performance fade. However, the time for CV for NCA batteries shows stability at the beginning of life.
4. Time for CV curiously decrease for the LFP technology.

High storage temperature (60 °C) impacted mainly the batteries which contained manganese in their chemistry, namely the LMO and the NMC. However, the LFP batteries demonstrate a very good resistance to this factor through aging time. Thus, the use of electrode materials which are more stable at high potential and high temperature is a major cause of prolonging battery life [24].

Furthermore, regarding the voltage window [$U_{min} - U_{max}$] of the four battery technologies, note that reducing this window and

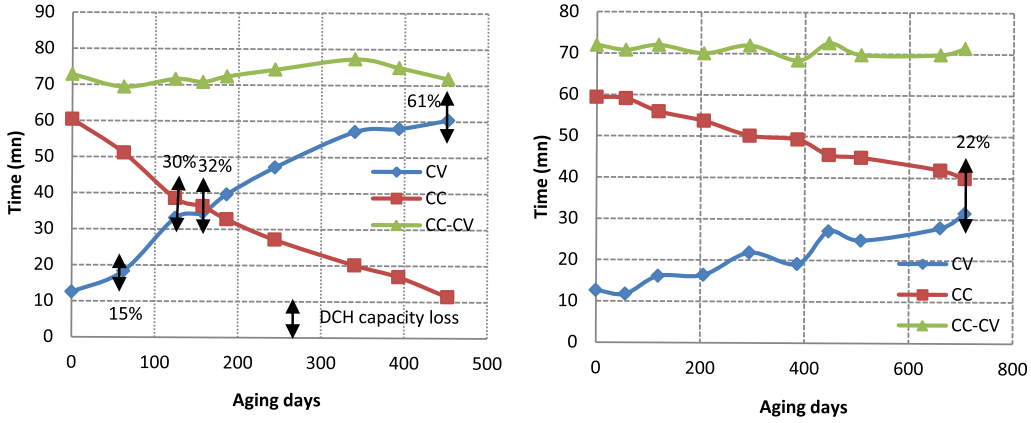

T60 and SOC100% *T45 and SOC100%*

Fig. 4. Time for CC, CV and global CC–CV charge through aging for NMC batteries from Kokam.

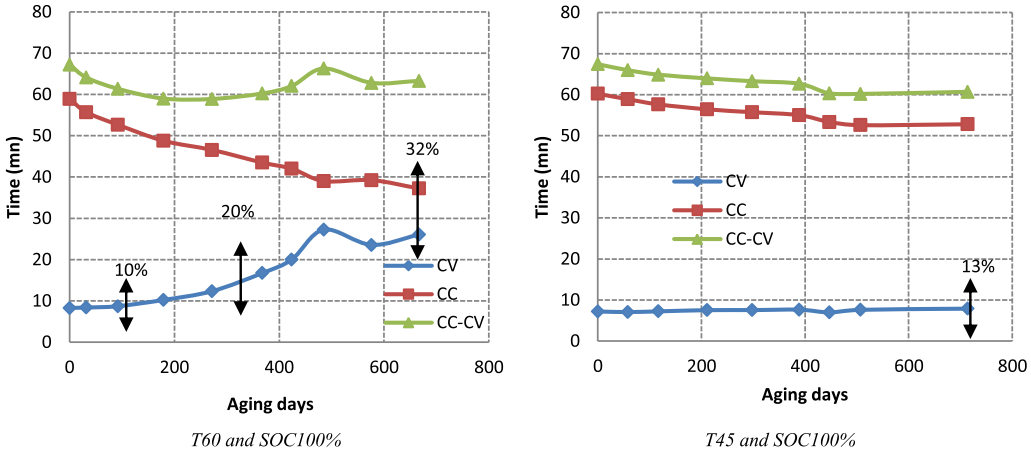

Fig. 5. Time for CC, CV and global CC–CV charge through aging for NCA batteries from SAFT.

mainly the U_{max} will reduce the occurrence of the side reaction and thus reduce the SEI resistance increase.

4. Constant voltage CV charge and electrochemical phenomena in lithium battery

4.1. Post mortem analysis

Post mortem analysis provided in literature performed on several battery technologies confirmed that the major aging source is the loss of cyclable lithium by lithium consumption due to the formation of the SEI interface mainly at the negative electrode. Due to this irreversible reaction, not all cyclable lithium intercalates back into anode leading to decrease in lithium concentration in this electrode.

Therefore, here we address our investigation to lithium intercalation problem at the anode. As this phenomenon is present in charging mode, that's why we chose to investigate the battery CC–CV charge. However, should we concentrate mainly on CV mode?

4.2. Electrochemical reaction within lithium battery

Based on the famous "rocking chair" process, lithium ions ensure charge migration within battery due to the insertion–deinsertion of lithium ion phenomenon in electrode materials. These ions migrate between anode and cathode thanks to the electrolyte in which a porous dielectric, the separator, ensures electronic insulation and ion migration [25].

During aging, physicochemical battery properties degrade. Principally, aging impacts the charge holding ability of the electrode and the effective ionic conductivity of the electrolyte. This is due to ion concentration and electrode design change once the electrode/electrolyte interface grows mainly at negative [26].

Indeed, kinetic of electrochemical reactions within the battery is certainly impacted with aging. Reaction rate at both of electrodes becomes slower. For example, from the Nyquist plots given in Fig. 2, diffusion reactions lasts more time when battery becomes aged. This aspect is more visible on LMO and NMC batteries.

In effect, like electrode porosity is affected, its surface area is reduced as well [27]. Moreover, electrolyte conductivity degradation leads principally to a charge transfer deceleration [28].

It is generally assumed that lithium intercalation/deintercalation takes place only at the solid electrode/electrolyte interface and this follows the Butler–Volmer equation given in (1),

$$I = Ai_0\left\{\exp\left[\frac{\alpha_a nF}{RT}(E - E_{eq})\right] - \exp\left[-\frac{\alpha_c nF}{RT}(E - E_{eq})\right]\right\} \quad (1)$$

where I is the electrode current (A), A the electrode active surface area (m^2), i_0 the exchange current density (A m^{-2}), E the electrode potential (V), E_{eq} the equilibrium potential (V), T the absolute temperature (K), n the number of electrons involved in the electrode reaction, F the Faraday constant, R the universal gas constant,

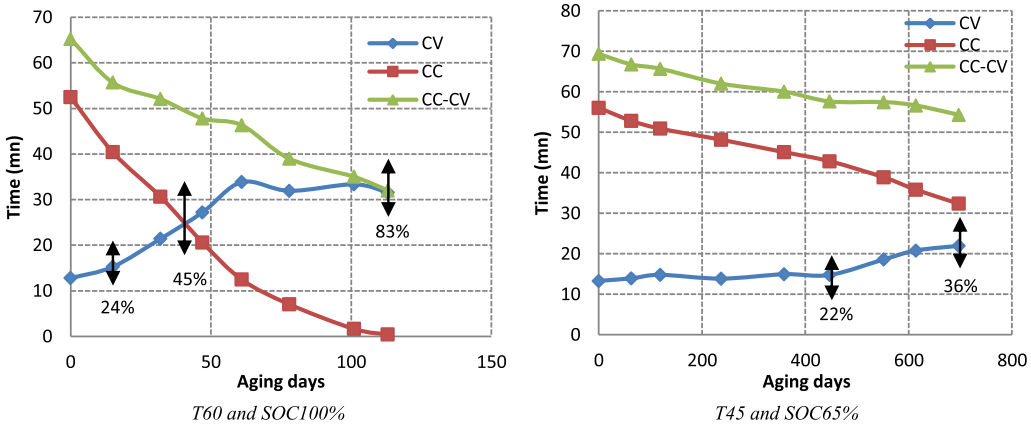

Fig. 6. Time for CC, CV and global CC–CV charge through aging for LMO batteries from LGChem.

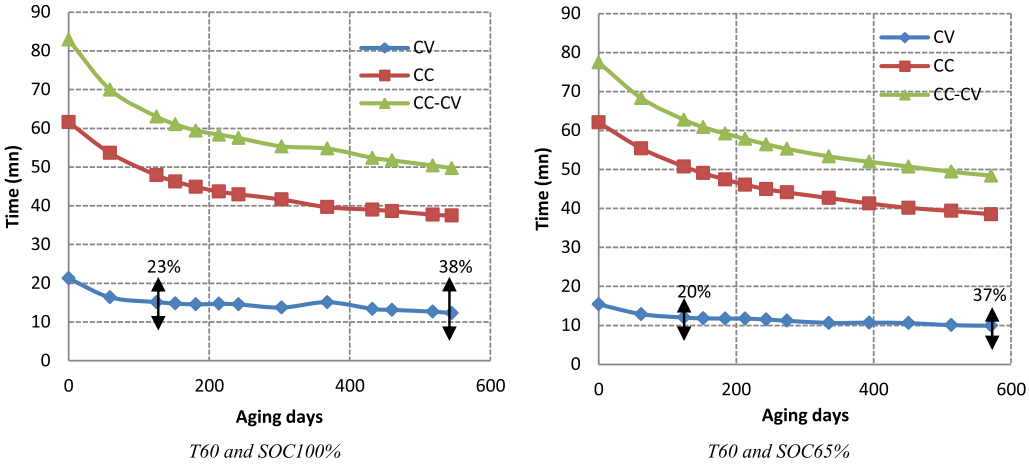

Fig. 7. Time for CC, CV and global CC–CV charge through aging for LFP batteries from LiFeBATT.

α_c the cathodic charge transfer coefficient and α_a the anodic charge transfer coefficient. The difference between the electrode potential and the equilibrium potential defines the activation overpotential given in (2).

$$\eta = (E - E_{eq}) \tag{2}$$

Activation overpotential participates in overall battery potential equilibrium referring to Nernst equation and it occurs mainly due to kinetic reactions and mass transfer when diffusion [26].

We assume that diffusion resulting from concentration gradients and migration caused by local electric field are responsible of ionic species transport in the electrolyte phase whereas diffusion is responsible of the transport of intercalated lithium in the solid phase. Furthermore, the active electrode materials are made from uniform spherical particles with a radius of R.

The equation that describes the diffusion of lithium in the solid phase of the electrodes is given by Fick's second law [29] (Eq. (3)),

$$\frac{\partial C_s(r)}{\partial t} = \frac{D_s}{r^2}\frac{\partial}{\partial r}\left(r^2\frac{\partial C_s(r)}{\partial r}\right) \tag{3}$$

where D_s is the diffusion coefficient in solid phase ($cm^2\ s^{-1}$) and C_s is the solid phase concentration of lithium (mol cm^{-3}).

When CC charge process begins, the applied current forces the lithium salt $LiPF_6$ move from the anode to the cathode; therefore it carries out a negative concentration gradient inside cathode, separator and anode [30]. Then, when the CC charge progresses, reversible lithium is transported from the cathode/electrolyte interface to the anode/electrolyte interface, the concentration gradient increases progressively along the current flow trail and reaches the maximum at the starting of the CV step, this indicates the end of the CC charge. Through the CV charge, the applied current drops rapidly, therefore leading the $LiPF_6$ concentration gradient to decrease from the maximum to a slight level as CV step reaches the end. Accordingly, system returns to a quasi-steady-state after cyclable lithium has intercalated back into anode [31].

This confirms that the CV step is responsible in a major part of lithium intercalation into negative electrode. Such a loss of cyclable lithium due to the SEI growth is more visible at this electrode, thus this confirms the significance of the CV phase investigation as state of health indicator. Ning et al. [31] confirmed this and they estimated that 5.5% of the cyclable lithium loss occurred during the CC charge mode, while 94.5% took place in the CV charge mode.

5. State of health determination based on kinetic of CV charge step

5.1. State of health determination based on battery current kinetic at CV step

Fig. 8 shows battery current during the CV step at several aging time for the LMO, NCA and NMC technologies and selected aging conditions (temperature and SOC). The several SOH are identified from calendar aging experiment longer than 22 months [32].

The simple expression (Eq. (4)) is used in order to simulate the battery current ($I(t)$) behavior through the CV step ($t = 0$ corresponding to the beginning of the constant voltage charging phase).

$$I(t) = Ae^{-Bt} + C \tag{4}$$

Current behavior at the CV step confirmed the exponential law with a good accuracy for all batteries and all check-ups. Fig. 9 illustrates examples of current model simulation at several check-ups for the LG, Kokam and SAFT batteries aged at SOC 100% and T 30 °C, T 45 °C and 60 °C respectively.

Table 2 reports the identified current model parameters through aging of the LMO battery aged following the test condition of T 30 °C and SOC 100% as well as the energy calculated during CC and CV phases respectively.

The identified model parameters through aging revealed to have a strong accordance to discharged capacity loss. Thus, taking into account relationship between model parameters and the capacity loss, Eq. (4) can be expressed as following:

$$I(t, c_{loss}) = A(c_{loss})e^{-B(c_{loss})t} + C(c_{loss}) \tag{5}$$

The process has been validated successfully on three major lithium-ion technologies (NCA, LMO and NMC) using aging data from several SOC and temperature conditions [32].

Particularly, B parameter is related to the battery capacity loss expressing its SOH with a linear function like given in Fig. 10 corresponding to three cases of Fig. 9 respectively. These examples are not exclusive. In any case, the identification quality criterion R^2 given by the method of least squares is very close to 1.

Considering the LMO technology and for all aging test conditions (couple of (SOC, T)), B parameter is quit constant at reduced capacity loss (less than 4%). However, when B reaches a defined threshold, that's means when intercalation becomes visibly very

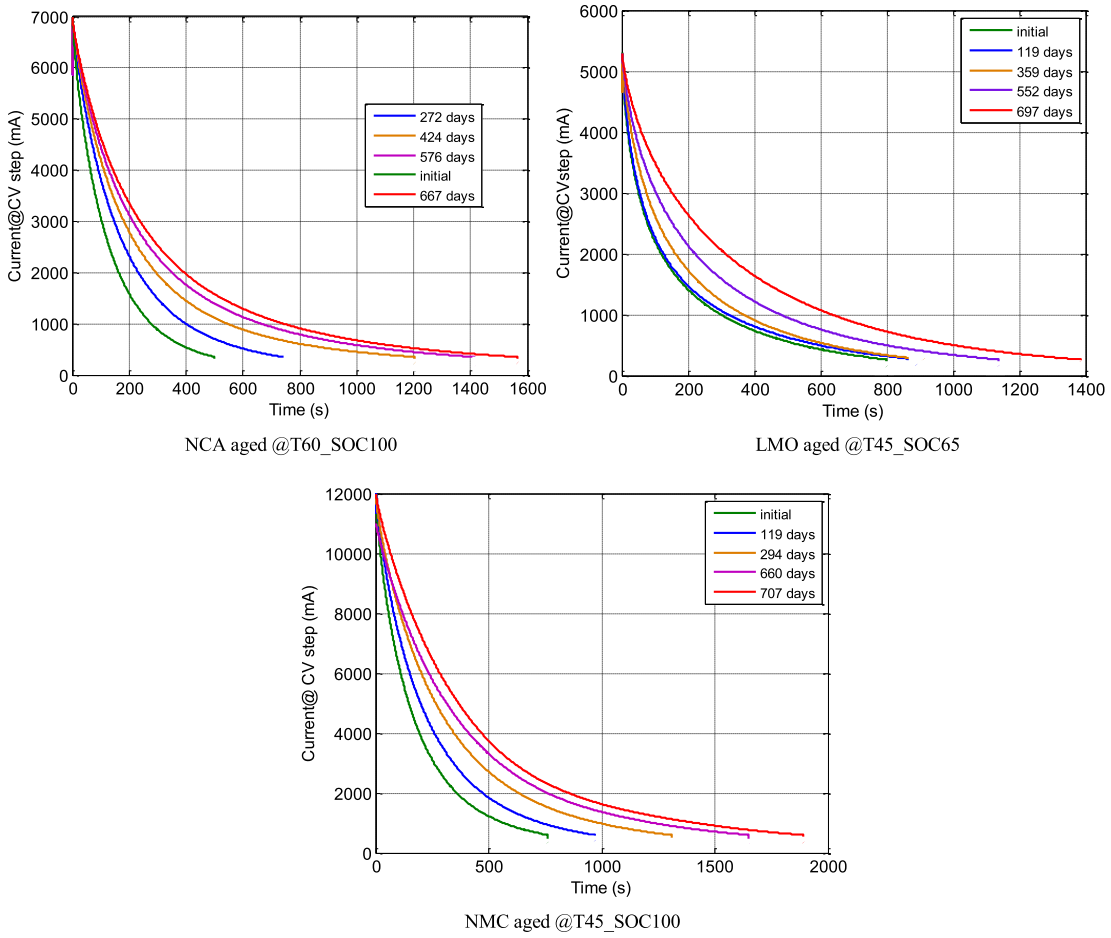

Fig. 8. Battery current evolution during the CV step at several aging time.

slow, there is an accurate linear relationship between B and the discharged capacity loss.

Thus, considering B parameter in the CV current model, we could extract rich information on intercalation time-constant and thus have indication on battery state of health. Moreover, this technique could provide accurate prediction of battery remaining useful life and thus allows having an on-board tool capable of battery capacity loss indication based only on time and current measurement during CC–CV recharge especially during the CV step [32]. The process of battery state of health tracking is summarized in Fig. 11. It consists of:

- A first constant-current charging phase,
- A second constant-voltage charging phase,
- A measure or a determination of, at least, one parameter characterizing the second phase (CV phase).
- SOH determination using this cited parameter and thanks to calibration.
- The calibration requires a reference method for determining the SOH of the battery. This method can be for example, a

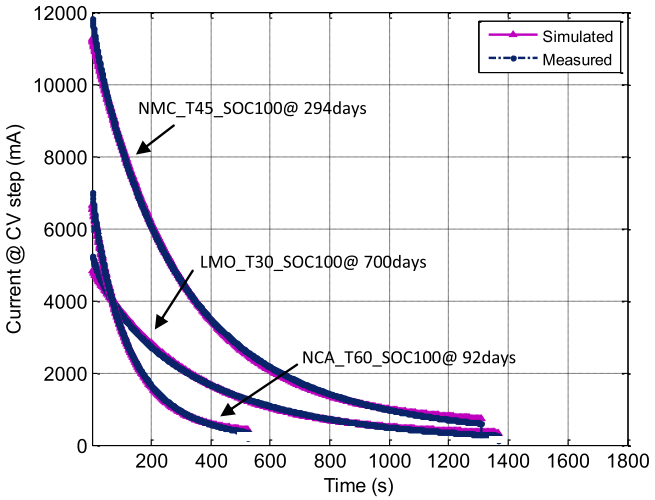

Fig. 9. Comparison between measured and simulated CV current for the NMC, NCA and LMO batteries aged at several conditions and after different aging days.

Table 2
Model parameters of the CV current at several aging time (LMO battery T30_SOC100).

Aging time/ parameters	A	B	C	Energy during CC (kW s)	Energy during CV (kW s)
0	3977.23	0.0074	396.93	60.036	3.61
61	3984.1	0.0078	411.46	60.705	3.564
121	4081.27	0.0079	405.2	58.736	3.421
232	4186.99	0.0069	382.27	55.454	3.812
361	4266.21	0.0055	348.72	51.522	4.563
455	4403.6	0.0047	332.35	47.764	5.369
535	4466.59	0.004	312.07	44.441	6.175
620	4542.83	0.0035	286.86	40.921	6.988
700	4620.13	0.003	258.03	37.055	8.053

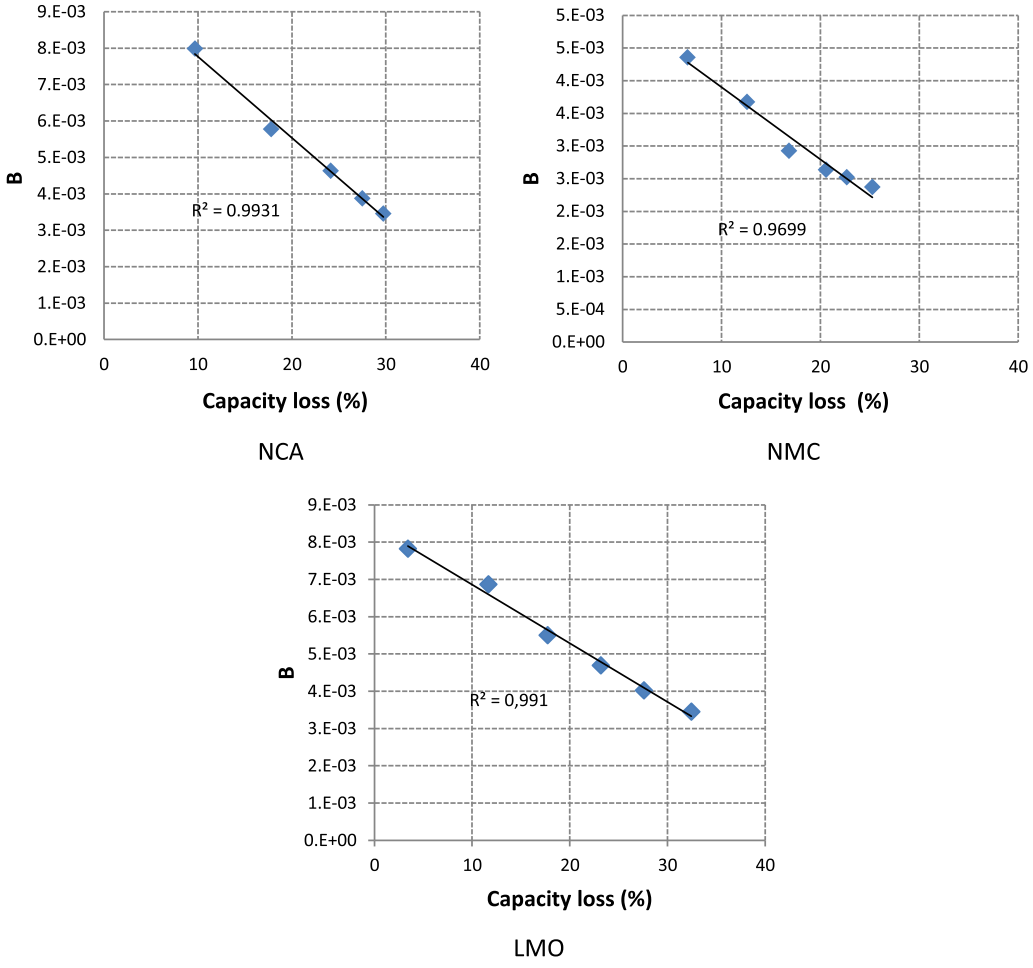

Fig. 10. Parameter B vs. aging quantified in terms of capacity loss for three batteries aged at several conditions.

measurement of the discharge capacity achieved at full battery discharge.

In order to have a reliable SOH determination, we suppose that the CC–CV charge is conducted at a controlled or at least a known temperature (for example 25 °C). The calibration allows taking into consideration the temperature impact on the relationship between the parameter characterizing the CV phase and the SOH.

Moreover, based on energy calculation during CV phase for several batteries SOH, we confirm the interest of this SOH determination approach. Fig. 12 shows the relative energy measured at CV step for the LMO battery aged at T 30 °C and SOC 100% which is calculated below,

$$E_{\text{relative}} = 100\left(\frac{E_t - E_{\text{ini}}}{E_{\text{ini}}}\right) \quad (6)$$

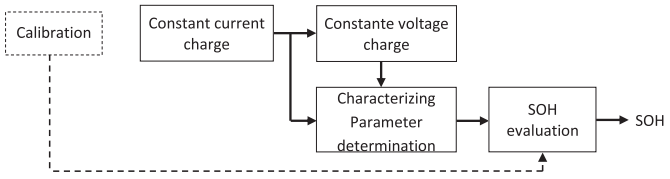

Fig. 11. State of health determination process based on CV step kinetic.

With the E_t the energy measured during the CV step in (W s) after t aging days and E_{ini} the initial value of such energy when battery still new.

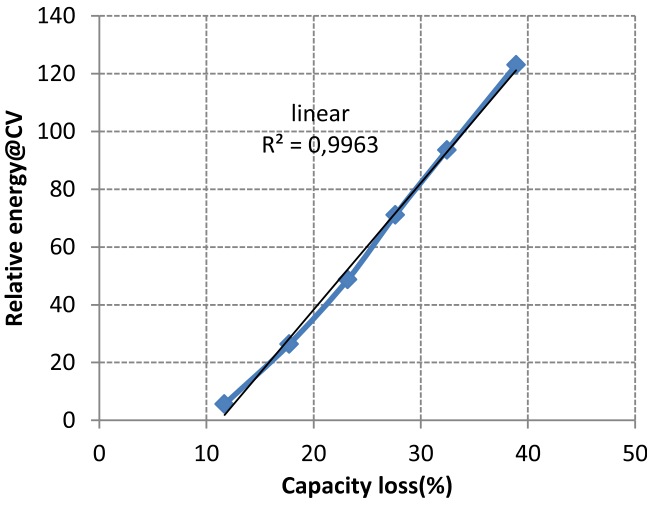

Fig. 12. Relative energy at CV phase vs. capacity loss.

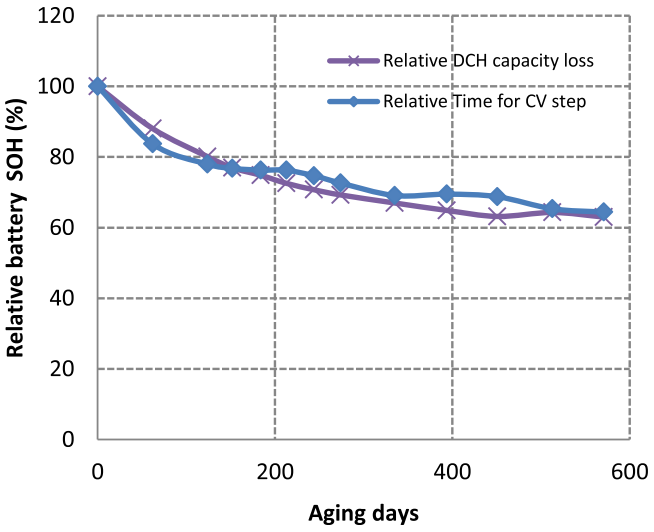

Fig. 13. Comparison between SOH estimation based on discharged capacity and time for CV charge for the LFP battery aged at *T* 60 °C and SOC 65%.

Thus, as another way to explore the CV phase for aging investigation and SOH determination, the parameter characterizing the CV phase can be the relative energy during this phase.

5.2. Investigation of the case of LFP battery

The approach described before showed a shortage to study the LFP technology. In fact, the time for CV for this kind of battery decreases continuously with aging.

However, the kinetic of CV phase confirmed again to be very interesting in order to study LFP battery SOH and based only on time of CV charge step calculation we achieved accurate estimation of LFP battery SOH compared to discharged capacity measurements. Fig. 13 shows a comparison between the relative SOH quantified in terms of discharged capacity and the relative SOH from time for CV charge step calculation for the LFP battery aged at *T* 60 °C and SOC 65%.

Results show that both of the curves are very similar. Thus, in this case, the SOH can be simply determined from a measurement of the CV phase duration.

Finally, the SOH determination process can be applied from each full battery recharge and thus a value of the SOH can be given according to full recharge frequency [32].

In all cases, the relationship between the parameter characterizing the CV charging phase may also be expressed using a correlation table instead of a linear or a nonlinear function.

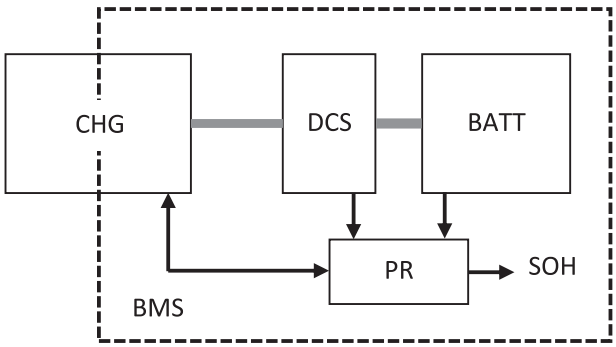

Fig. 14. Block diagram of the battery SOH-evaluating device.

Criteria of end of life of lithium-ion batteries or criteria of moving to a second life in some recent applications depend on the application requirement. Generally, this criterion is assumed around 20%–30% of capacity loss. Anyway, beyond a defined performance, battery will not be able to satisfy energy/power request so it will be replaced or it will be used in another application requiring less energy density and less power capability.

6. Method integration within battery management system: BMS

Fig. 14 gives a block diagram of a device conceived to implement our evaluating method of the battery state-of-health within a battery management system used for example in the case of an EV or a plug-in hybrid EV PHEV. This device is composed of a CC–CV conventional charger CHG used to charge the lithium-ion battery BATT. It contains also a device for charge supervising DCS and a tool for data processing PR. The DCS includes for example current and voltage sensors used in order to measure the battery current *I* and the battery voltage *U* respectively. Moreover, the DCS can be integrated in the charger or in the battery.

The data processor PR (a digital processor or an electronic card holding such a processor) is programmed and/or configured to exploit measurements received from the DCS in order to determine the battery SOH using the method discussed previously. This processor can also control the charger CHG, for example it can control the transition between CC and CV charging steps or control the end of charge when the current *I* reaches the minimal value I_{min} [32].

7. Conclusion

This work focus on calendar aging of lithium batteries based on charge kinetic during periodic characterization protocols. The identification of the time for CC–CV charge demonstrates different behavior for the four batteries technologies. Mainly the kinetic for CV charge step served as an indicator of lithium battery state of health.

According to lithium battery technologies, the current during CV charge step has been useful for NMC, NCA and LMO battery SOH determination. However, in the case of LFP battery a simple calculation of the duration of the CV step revealed to be very accurate compared to the classic discharged capacity measurement.

Finally, this study could help to simplify SOH algorithm used in battery management system. Moreover, it could be very useful to charge problem investigations such as precise cost calculation and optimization.

Acknowledgments

This work was funded by the French National Research Agency (ANR) under the SIMCAL research program. SIMCAL network partners are CEA, EDF, EIGSI, IFP-EN, IFSTTAR, IMS, LEC, LMS-Imagine, LRCS, PSA, RENAULT, SAFT, VALEO.

References

[1] L. Lu, X. Han, J. Li, J. Hua, M. Ouyang, J. Power Sources 226 (2013) 272–288.
[2] J. Zhang, J. Lee, J. Power Sources 196 (2011) 6007–6014.
[3] C.D. White, K.M. Zhang, J. Power Sources 196 (2011) 3972–3980.
[4] A. Eddahech, O. Briat, N. Bertrand, J.-Y. Delétage, J.-M. Vinassa, Int. J. Electr. Power Energy Syst. 42 (1) (2012) 487–494.
[5] T. Osaka, T. Momma, D. Mukoyama, H. Nara, J. Power Sources 205 (2012) 483–486.
[6] T. Hang, D. Mukoyama, H. Nara, N. Takami, T. Momma, T. Osaka, J. Power Sources 222 (2013) 442–447.
[7] A. Eddahech, O. Briat, H. Henry, J.-Y. Delétage, E. Woirgard, J.-M. Vinassa, Microelectron. Reliab. 51 (9–11) (2011) 1968–1971.

[8] W.X. Shen, C.C. Chan, E.W.C. Lo, K.T. Chau, Energy Convers. Manag. 43 (6) (2002) 817–826.
[9] S. Wang, M. Verbrugge, J.S. Wang, P. Liu, J. Power Sources 196 (2011) 8735–8741.
[10] A. Eddahech, O. Briat, J.M. Vinassa, in: Proc. IEEE Energy Conversion Congress and Exposition Conf, 2012. Raleigh, North Carolina.
[11] H. Jannesaria, M.D. Emamia, C. Ziegler, J. Power Sources 196 (2011) 9654–9664.
[12] J. Remmlinger, M. Buchholz, T. Soczka-Guth, K. Dietmayer, J. Power Sources 239 (2013) 689–695.
[13] B.Y. Liaw, R.G. Jungst, G. Nagasubramanian, H.L. Case, D.H. Doughty, J. Power Sources 140 (2005) 157–161.
[14] M.A. Roscher, J. Assfalg, O.S. Bohlen, IEEE Trans. Veh. Technol. 60 (1) (2011) 98–103.
[15] C. Guenther, B. Schott, W. Hennings, P. Waldowski, M.A. Danzer, J. Power Sources 239 (2013) 604–610.
[16] M. Fleckenstein, S. Fischer, O. Bohlen, B. Bäker, J. Power Sources 223 (2013) 259–267.
[17] A. Eddahech, O. Briat, J.M. Vinassa, E. Woirgard, Microelectron. Reliab. 52 (2012) 2438–2442.
[18] S.C. Nagpure, R.G. Downing, B. Bhushan, S.S. Babud, Scr. Mater. 67 (2012) 669–672.
[19] S.C. Nagpure, R.G. Downing, B. Bhushan, S.S. Babu, L. Cao, Electrochim. Acta 56 (2011) 4735–4743.
[20] J. Vetter, P. Novak, M.R. Wagner, C. Veit, K.-C. Moller, J.O. Besenhard, M. Winter, M. Wohlfahrt-Mehrens, C. Vogler, A. Hammouche, J. Power Sources 147 (2005) 269–281.
[21] A. Eddahech, O. Briat, J.M. Vinassa, Electrochim. Acta 114 (2013) 750–757.
[22] E. Jacques, M.H. Kjell, D. Zenkert, G. Lindbergh, M. Behm, M. Willgert, Compos. Sci. Technol. 72 (2012) 792–798.
[23] P. Ramadass, B. Haran, P.M. Gomadam, R. White, B.N. Popov, J. Electrochem. Soc. 151 (2004) 196–203.
[24] A. Eddahech, O. Briat, J.M. Vinassa, Energy 61 (2013) 432–439.
[25] S. Raël, M. Hinaje, J. Power Sources 222 (2013) 112–122.
[26] S. Sankarasubramaniana, B. Krishnamurthy, Electrochim. Acta 70 (2012) 248–254.
[27] D. Linden, T.B. Reddy, Handbook of Batteries, 2002, pp. 41–42.
[28] M. Kassem, C. Delacourt, J. Power Sources 235 (2013) 159–171.
[29] Y. Ye, Y. Shi, N. Cai, J. Lee, X. He, J. Power Sources 199 (2012) 227–238.
[30] S. Bashash, S.J. Moura, J.C. Forman, H.K. Fathy, J. Power Sources 196 (2011) 541–549.
[31] G. Ning, R.E. White, B.N. Popov, Electrochim. Acta 51 (2006) 2012–2022.
[32] A. Eddahech, O. Briat, J.M. Vinassa, Method and Device for State of Health Quantification of Lithium-ion Batteries Based on Constant Voltage Charging Phase, French Patent 13/59508 FR, October 1st, 2013.